XLVI CILAMCE
VITÓRIA - ES - BRAZIL - 2025
XLVI IBERO-LATIN AMERICAN CONGRESS ON COMPUTATIONAL METHODS IN ENGENEERING

On the Effects of Consistent Stabilization Techniques and a Turbulence Model for Fluid–Structure Interaction

Matheus Haubert Yokomizo[1], Jeferson Wilian Dossa Fernandes[2], Rodrigo Ribeiro Paccola[1], Rodolfo André Kuche Sanches[1]

[1]*Structural Engineering Department, University of São Paulo (USP)*
Av. Trab. São Carlense, 400, São Carlos, Brazil
matheus_haubert@usp.br, rpaccola@sc.usp.br, rodolfo.sanches@usp.br
[2]*Structural Engineering Department, Federal University of Minas Gerais (UFMG)*
Av. Presidente Antônio Carlos, 6627, Pampulha, Belo Horizonte, Brazil
jwdfernandes@ufmg.br

Abstract. Fluid-structure interaction (FSI) is a key phenomenon in many engineering applications, characterized by the mutual influence of motion and forces between the fluid and the solid domains. Numerical simulations of FSI problems using the Finite Element Method (FEM) often face challenges related to stability and convergence of the fluid dynamics problem, such as spurious oscillations in convection-dominated regimes and pressure instabilities in incompressible flows. Additionally, high Reynolds number flows introduce turbulence effects that can hinder convergence and require fine discretizations, significantly increasing computational cost. To address these challenges while maintaining representative results, several stabilizing techniques and turbulence modeling strategies have been proposed in the literature. This work presents a comparative analysis of consistent stabilized formulations for incompressible flows with vorticity interacting with flexible structures. It includes the Streamline-Upwind/Petrov-Galerkin (SUPG), Pressure-Stabilized Petrov-Galerkin (PSPG), and Variational Multiscale (VMS) techniques. The influence of incorporating a Large-Eddy Simulation (LES) turbulence model is also examined. The fluid flow is described within the Arbitrary Lagrangian–Eulerian (ALE) framework and coupled with a large-displacement structural mechanics solver using a strong partitioned approach. Time integration is performed using the generalized-α method, and the fluid mesh motion is governed by the Laplace equation. The results showed that the SUPG/PSPG formulation did not reach the long-term response, while the VMS method performed better. The inclusion of LES significantly improved the results, especially for the SUPG/PSPG simulation.

Keywords: Fluid-Structure interaction, Stabilization techniques, Large-Eddy Simulation, Vorticity

1 Introduction

Fluid–structure interaction (FSI) problems involve the mutual coupling between a flowing fluid and a flexible structure immersed within it. The numerical analysis of such problems is particularly challenging due to the interaction of domains governed by different constitutive models, physical properties, and distinct degrees of freedom. This coupling demands specialized numerical techniques to ensure both the stability and accuracy of the solution.

Among the available approaches for simulating FSI problems, the Finite Element Method (FEM) stands out for its flexibility and ability to handle complex geometries. However, its application to computational fluid dynamics (CFD) presents challenges related to numerical stability, such as spurious oscillations in convection-dominated flows and restriction in the choice of approximation spaces for velocity and pressure in incompressible flows to avoid instabilities in the pressure field. To overcome these difficulties and improve the robustness of the method, several stabilization techniques have been proposed, including the Streamline-Upwind/Petrov–Galerkin (SUPG) method [1], the Pressure-Stabilized Petrov–Galerkin (PSPG) method [2], and the Variational Multiscale Method (VMS) [3–5].

Another challenge arises at high Reynolds numbers, where the flow transitions from laminar to turbulent. In this regime, three-dimensional, chaotic vortical structures form across a wide range of spatial and temporal scales, making the direct numerical simulation (DNS) computationally prohibitive due to the need for extremely refined meshes and small time steps. To overcome this problem, several turbulence models have been developed, such as the Reynolds-Averaged Navier–Stokes (RANS) [6] and the Large Eddy Simulation (LES) [7] approaches, which

enable more computationally efficient simulations.

Furthermore, the CFD formulation must account for the motion of the structure. To achieve this, two main strategies are commonly employed: fixed-mesh methods [8] and moving-mesh methods [9]. The latter requires a formulation of the governing equations that allows the mesh to deform, which can be accomplished using the Arbitrary Lagrangian–Eulerian (ALE) framework [10]. The ALE formulation enables the reference domain to move independently of both the material and spatial domains, making it particularly well-suited for fluid–structure interaction problems. In this context, an additional model is required to govern the dynamic deformation of the mesh, ensuring its conformity to the deformed structure [11].

Regarding the solid dynamics, FSI problems ofter demand nonlinear geometric analysis due to large displacement effects [11, 12].

Finally, the coupling between the different subproblems – solid, fluid, and mesh motion – must be addressed. A consistent strategy is the monolithic approach, in which all governing equations are solved simultaneously in a single system. However, this method lacks flexibility and can limit the applicability of different solvers for each subproblem. An alternative is the partitioned approach, where each subproblem is solved independently, and their interaction is managed through an iterative procedure. This scheme offers greater modularity and flexibility, particularly when incorporating new elements or extending existing implementations.

Thus, this work presents a study of FSI problems, evaluating the performance of different stabilization techniques and the influence of the Large Eddy Simulation (LES) turbulence model. The fluid flow is solved using the Arbitrary Lagrangian–Eulerian (ALE) description, while the structural domain is treated with a total Lagrangian formulation. The coupling between fluid and structure is carried out using a strongly partitioned scheme.

2 Computational solid dynamics formulation

The computational solid dynamics problem is solved using the Finite Element Method (FEM) in a total Lagrangian framework for Reissner-Mindlin shells with the Saint-Venant-Kirchhoff constitutive model. The shell finite element is chosen because it can represent most of the 3D FSI problems at a better computational cost than solid elements. We adopt the positional formulation for shells as proposed by [13] and later successfully applied to dynamics and FSI problems in [11, 12] using the Newmark-β time integrator. In this work, to ensure consistency between the numerical formulations adopted for the structural and fluid domains, the generalized-α time integration scheme is adopted for both problems.

In this formulation, the intial ($\boldsymbol{x}$) and current ($\boldsymbol{y}$) shell coordinates are mapped respectively according to:

$$\boldsymbol{x}(\boldsymbol{\xi}) = \sum_{a=1}^{n_{\text{en}}} \left[\boldsymbol{x}_a^{\text{m}} N_a(\xi_1, \xi_2) + \frac{h_0}{2} \boldsymbol{v}_a^0 N_a(\xi_1, \xi_2) \xi_3 \right], \tag{1a}$$

$$\boldsymbol{y}(\boldsymbol{\xi}) = \sum_{a=1}^{n_{\text{en}}} \left[\boldsymbol{y}_a^{\text{m}} N_a(\xi_1, \xi_2) + \frac{h_0}{2} \boldsymbol{v}_a^1 N_a(\xi_1, \xi_2) \left(\xi_3 + \sum_{b=1}^{n_{\text{en}}} \alpha_b N_b(\xi_1, \xi_2) \xi_3^2 \right) \right], \tag{1b}$$

where the subindexes a and b refer to the node number, n_{en} is the number of element nodes in the element, $\boldsymbol{\xi}$ are the parametric nondimensional coordinates, h_0 is the initial shell thickness, $N_a(\xi_1, \xi_2)$ is the shape function associated with node a, $\boldsymbol{x}^{\text{m}}$ and $\boldsymbol{y}^{\text{m}}$ are the initial and current coordinates of the mid-surface, respectively, $\boldsymbol{v}^0$ and $\boldsymbol{v}^1$ are the generalized vectors in the initial (unity and normal to the middle surface) and current configurations, respectively. α is an additional parameter introduced to account for the linear rate of thickness variation. These values are schematically represented in Figure 1.

As mentioned, the problem is discretized in time with the generalized-α and the solution is obtained through an implicit energetic approach as presented in [12].

3 Computational fluid dynamics formulation

The computational fluid dynamics (CFD) problem addressed in this work concerns incompressible Navier-Stokes flows, which, in the ALE description are governed by the balance of linear momentum equation (Eq. (2a)) and the mass conservation equation (continuity – Eq. (2b)):

$$\rho \left(\left. \frac{\partial \boldsymbol{u}}{\partial t} \right|_{\hat{\boldsymbol{x}}} + ((\boldsymbol{u} - \hat{\boldsymbol{u}}) \cdot \boldsymbol{\nabla}) \boldsymbol{u} - \boldsymbol{f} \right) - \boldsymbol{\nabla} \cdot \boldsymbol{\sigma} = \boldsymbol{0} \text{ in } \Omega, \tag{2a}$$

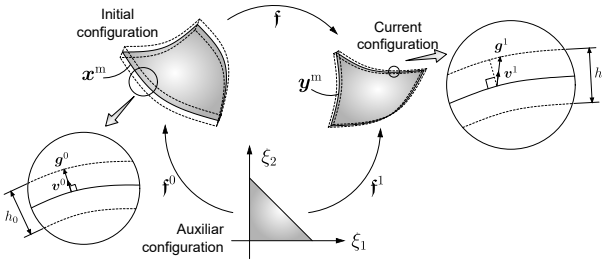


Figure 1. Shell kinematic and generalized vector.

$$\boldsymbol{\nabla} \cdot \boldsymbol{u} = 0 \text{ in } \Omega, \tag{2b}$$

in which $\boldsymbol{u}$ is the fluid velocity, $\hat{\boldsymbol{u}}$ is the mesh velocity, ρ is the fluid density, $\boldsymbol{f}$ is the body force by unit mass and $\boldsymbol{\sigma}$ is the Cauchy stress tensor, given by $\boldsymbol{\sigma} = 2\mu\dot{\boldsymbol{\varepsilon}} - p\mathbf{I}$, where μ is the dynamic viscosity, p is the pressure field, $\mathbf{I}$ is the identity tensor, $\dot{\boldsymbol{\varepsilon}} = (\boldsymbol{\nabla}\boldsymbol{u} + (\boldsymbol{\nabla}\boldsymbol{u})^{\mathrm{T}})/2$ is the strain rate tensor.

The semi-discrete problem, using finite elements, is obtained trough the weighted residual method. Following the Galerkin technique, it results the following equations for momentum and continuity, respectively:

$$\int_\Omega N_a^u \rho \left(\left.\frac{\partial \boldsymbol{u}^h}{\partial t}\right|_{\hat{\boldsymbol{x}}} + \left((\boldsymbol{u}^h - \hat{\boldsymbol{u}}^h) \cdot \boldsymbol{\nabla} \right) \boldsymbol{u}^h - \boldsymbol{f}^h \right) d\Omega + \int_\Omega \boldsymbol{\sigma}^h \cdot \boldsymbol{\nabla} N_a^u d\Omega - \int_{\Gamma_N} N_a^u \boldsymbol{h}^h d\Gamma_N = \mathbf{0} \text{ and} \tag{3a}$$

$$\int_\Omega N_a^p \boldsymbol{\nabla} \cdot \boldsymbol{u}^h d\Omega = 0, \tag{3b}$$

in which Γ_N is the Neumann boundary, where traction ($\boldsymbol{h}$) is applied, N_a^u and N_a^p denotes, respectively, the velocity and pressure shape functions associated with node a. The superscript h indicates variables approximated by the finite space of functions.

However, the Galerkin formulation can lead to instabilities in the solution due to the convective terms and to inadequate combination of velocity and pressure shape functions [14, 15]. Therefore, in the present work, the stabilized SUPG/PSPG formulation, according to Tezduyar [16], is used. In this formulation, the residue of the momentum equation is weighted by two different specially designed functions resulting and added to the weak form of momentum equation and to the weak form of continuity equation. The portions that are added to (3a) and (3b) are, respectively:

$$+\sum_{e=1}^{n_{\mathrm{el}}} \int_{\Omega^e} \tau_{\mathrm{SUPG}} (\boldsymbol{u}^h - \hat{\boldsymbol{u}}^h) \cdot \boldsymbol{\nabla} N_a^u \cdot \boldsymbol{r}_{\mathrm{M}}(\boldsymbol{u}^h, p^h) d\Omega^e \text{ and} \tag{4a}$$

$$+\sum_{e=1}^{n_{\mathrm{el}}} \int_{\Omega^e} \tau_{\mathrm{PSPG}} \frac{\boldsymbol{\nabla} N_a^p}{\rho} \cdot \boldsymbol{r}_{\mathrm{M}}(\boldsymbol{u}^h, p^h) d\Omega^e. \tag{4b}$$

The parameters τ_{PSPG} and τ_{SUPG} are designed to ensure good convergence. In this work we adopt $\tau_{\mathrm{PSPG}} = \tau_{\mathrm{SUPG}}$, calculated according to [17].

Another stabilization term that can be incorporated into the formulation is the Least-Squares on the Incompressibility Constraint (LSIC), which adds the following term to eq. (3a):

$$+\sum_{e=1}^{n_{\mathrm{el}}} \int_{\Omega^e} \rho \nu_{\mathrm{LSIC}} \boldsymbol{\nabla} N_a^u r_{\mathrm{C}} d\Omega^e. \tag{5}$$

3.1 Variational Multiscale Method

The variational multiscale (VMS) [3–5] method is based on the decomposition of the solution fields into resolved (large-scale) components and unresolved (small-scale) components. This separation enhances numerical

stability and accuracy in the simulation, since it inherently incorporates SUPG/PSPG stabilization, in addition to introducing additional terms, ensuring consistency and stability.

The VMS method adds to eq. (3a) and eq. (3b) the terms given by eq. (6a) and eq. (6b), respectively:

$$\begin{aligned}\sum_{e=1}^{n_{\mathrm{el}}}\int_{\Omega^e}\tau_{\mathrm{SUPS}}(\boldsymbol{u}^h-\hat{\boldsymbol{u}}^h)\cdot\boldsymbol{\nabla}N_a^u\cdot\boldsymbol{r}_{\mathrm{M}}d\Omega^e+\sum_{e=1}^{n_{\mathrm{el}}}\int_{\Omega^e}\rho\nu_{\mathrm{LSIC}}\boldsymbol{\nabla}N_a^u r_{\mathrm{C}}d\Omega^e-\\ \sum_{e=1}^{n_{\mathrm{el}}}\int_{\Omega^e}\tau_{\mathrm{SUPS}}N_a^u\left((\boldsymbol{r}_{\mathrm{M}}\cdot\boldsymbol{\nabla})\,\bar{\boldsymbol{u}}\right)d\Omega^e-\sum_{e=1}^{n_{\mathrm{el}}}\int_{\Omega^e}\frac{\boldsymbol{\nabla}N_a^u}{\rho}\cdot(\tau_{\mathrm{SUPS}}\boldsymbol{r}_{\mathrm{M}})\otimes(\tau_{\mathrm{SUPS}}\boldsymbol{r}_{\mathrm{M}})d\Omega^e,\end{aligned} \tag{6a}$$

$$+\sum_{e=1}^{n_{\mathrm{el}}}\int_{\Omega^e}\tau_{\mathrm{SUPS}}\frac{\boldsymbol{\nabla}N_a^p}{\rho}\cdot\boldsymbol{r}_{\mathrm{M}}d\Omega^e. \tag{6b}$$

In this formulation, τ_{SUPS} is a stabilizing parameter, computed according to [17].

3.2 Time integration

As previously mentioned in Section 2, the time integration scheme adopted is the generalized-α method [18]. This method is particularly effective as it allows for straightforward control of the numerical dissipation introduced by the integrator through a single arbitrary parameter, providing optimal dissipation of high frequencies.

3.3 Large-Eddy Simulation

The Large-Eddy Simulation (LES) turbulence model [7] is an effective approach for simulating high Reynolds number flows, enabling the use of coarser meshes while still capturing the essential flow features. In this work, the Smagorinsky eddy-viscosity model is adopted, so that we add the following term to eq. (3a):

$$+\sum_{e=1}^{n_{\mathrm{el}}}\int_{\Omega^e}2\rho\nu_T\,(\dot{\bar{\boldsymbol{\varepsilon}}}\cdot\boldsymbol{\nabla}N_a^u)d\Omega^e, \tag{7}$$

where $\nu_T=(C_S\Delta)^2\left\|\dot{\bar{\boldsymbol{\varepsilon}}}\right\|$ is the eddy viscosity, C_S is the Smagorinsky constant, Δ is the filter width, $\dot{\bar{\boldsymbol{\varepsilon}}}$ is the strain rate tensor of the filtered component, with norm $\left\|\dot{\bar{\boldsymbol{\varepsilon}}}\right\|=(2\dot{\bar{\boldsymbol{\varepsilon}}}:\dot{\bar{\boldsymbol{\varepsilon}}})^{1/2}$.

4 Fluid-Structure interaction

FSI problems must satisfy three fundamental coupling conditions [11, 17, 19]: (1) the kinematic condition, which enforces the continuity of velocities at the interface; (2) the dynamic condition, which requires the continuity of tractions at the interface; and (3) the geometric condition, which imposes compatibility between the geometries of the domains at the interface, preventing the formation of gaps or overlaps.

On the other hand, different coupling strategies can be employed, such as: the monolithic approach, in which all subproblems are solved simultaneously within a single system of equations; or partitioned approaches, where these subproblems are solved separately, with their interactions enforced through appropriate transmition of boundary conditions at the fluid-structure interface. The latter approach enables the use of codes developed independently for each subdomain, facilitating the coupling of different types of elements and making it easier to identify potential implementation errors.

In this work, a strong partitioned coupling approach is employed, in which the solution for the coupled fluid, structural, and mesh dynamic problems is obtained through a block-iterative scheme within Newton Raphson method.

The mesh movement scheme adopted in this work is based on the Laplace equation, in a similar approach to [20, 21].

4.1 Numerical example

To perform this study, we consider a problem originally proposed by Wall and Ramm [22], which has been widely used for assessing numerical methods for FSI. This problem consists of a flexible panel clamped at one end to a rigid block subjected to an incompressible flow, as shown in Fig. 2.

The fluid computational domain has dimensions of $21.0 \times 12.0 \times 4.0$ cm³, density $\rho_f = 1.18 \times 10^{-3}$ g/cm³ and dynamic viscosity $\mu = 1.82 \times 10^{-4}$ g/(cm·s). The flexible panel has a length of 4 cm, thickness of 0.06 cm, Young's modulus $E = 2.5 \times 10^6$ g/(cm·s²), density $\rho_s = 0.1$ g/cm³, and zero Poisson's ratio, as adopted by [11]. The inflow velocity is prescribed as $u_\infty = 51.3$ cm/s at the left boundary. Slip boundary conditions are enforced along the top, bottom, frontal and back walls, traction-free ($\boldsymbol{h} = \mathbf{0}$) condition is applied at the right boundary and no-slip conditions is considered at the FSI interface and rigid block walls.

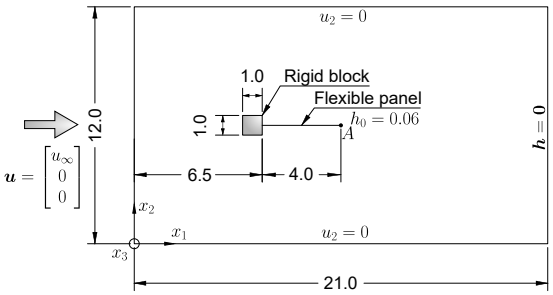


Figure 2. Flag flutter – Schematic drawing (Dimensions in cm).

Time integration was carried out using the generalized-α method with a spectral radius of $\varrho_\infty = 0.0$ and a time step of $\Delta t = 1.65 \times 10^{-3}$ s, over the interval $t \in [0.0,\ 5.0]$ s. The mesh for the fluid domain discretization consists of $6,794$ quadratic tetrahedral elements, $11,806$ nodes, and $47,224$ degrees of freedom. The shell mesh consists of 200 quadratic triangular elements, 441 nodes, and $3,087$ degrees of freedom. Figure 3 shows the spatial discretization for both domains. The transfer of coupling conditions between the different problems is performed directly, which implies that the nodes at the interaction interface are coincident.

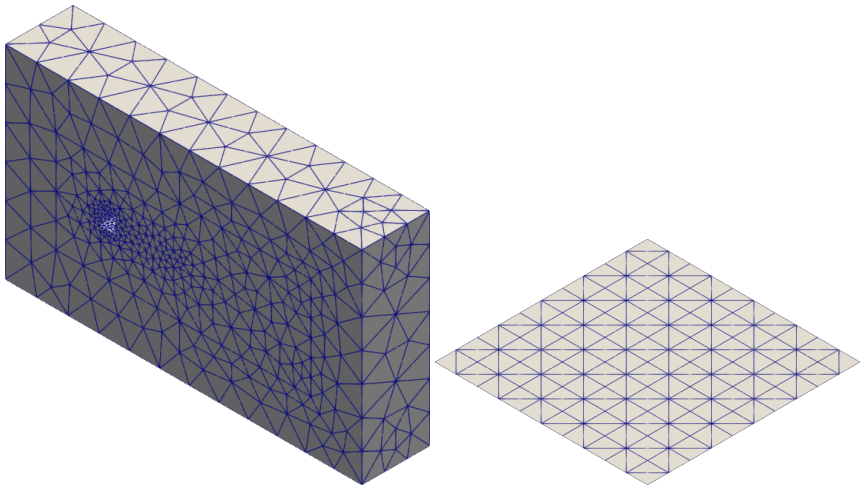


Figure 3. Flag flutter – Left: Fluid mesh; Right: Shell mesh.

Numerical simulations were conducted using both the SUPG/PSPG and VMS stabilized formulations, considering cases without turbulence modeling (Direct Numerical Simulation – DNS) and with the inclusion of the LES turbulence model.

Figure 4 shows the vertical displacement of point A, at the tip of the panel, over time for all simulations. These results are summarized in Table 1. Comparing with the results of [22], who reported an oscillation period of 0.33 s, equivalent to a frequency of 3 Hz, it was observed that the simulation using the SUPG/PSPG formulation without LES did not reach the long-term response, exhibiting a very low rate of increase in displacement amplitude.

In contrast, the simulations incorporating the LES turbulence model were able to adequately capture the structural behavior. Additionally, the VMS formulation without LES also provided a satisfactory description of the structure's response.

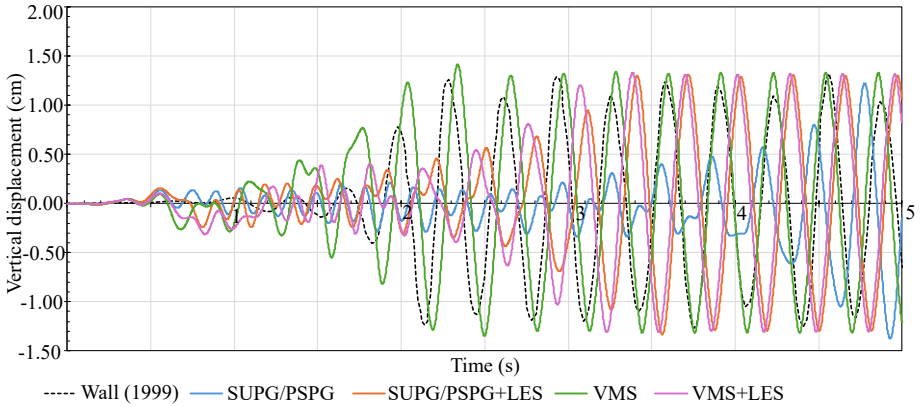


Figure 4. Flag flutter – Tip vertical displacement.

Table 1. Amplitude and frequencies in each simulation.

Model	Amplitude (cm)	Period (s)	Frequency (Hz)
SUPG/PSPG	–	–	–
SUPG/PSPG+LES	1.379	0.330	3.028
VMS	1.358	0.315	3.179
VMS+LES	1.384	0.327	3.062

5 Conclusions

In this work, in the context of finite element analysis of fluid-structure interaction, we implement the stabilized formulations SUPG/PSPG, the VMS method and the LES turbulence model and study the effects of each model in the simulation of a fluid-structure interaction problem. The structure is modeled trough a large displacement total Lagrangian formulation for Reissner-Mindlin shells and the fluid mesh movement is performed using the Laplace equation. The fluid-structure coupling is performed using a strong partitioned scheme.

The numerical example demonstrated that the SUPG/PSPG stabilization model did not reach the long-term response, while the VMS formulation provided more satisfactory results. Incorporating the LES turbulence model significantly improved the outcomes, particularly for the SUPG/PSPG-stabilized simulation.

For future works, additional studies should be performed with different mesh refinement levels and higher Reynolds numbers to enable a more comprehensive assessment of the impact of the stabilization and turbulence models on the results of the coupled problem.

Acknowledgements. The authors gratefully acknowledge the financial support provided by the Coordination for the Improvement of Higher Education Personnel (CAPES) – Finance Code 001, the National Council for Scientific and Technological Development (CNPq) – grants 131191/2022-5 and 314045/2023-6, the São Paulo Research Foundation (FAPESP) – grant 2024/05554-9, and the Research Support Foundation of the State of Minas Gerais (FAPEMIG) – grant APQ-01099-24.

Authorship statement. The authors hereby confirm that they are the sole liable persons responsible for the authorship of this work, and that all material that has been herein included as part of the present paper is either the property (and authorship) of the authors, or has the permission of the owners to be included here.

References

[1] A. N. Brooks and T. J. Hughes. Streamline upwind/petrov-galerkin formulations for convection dominated flows with particular emphasis on the incompressible navier-stokes equations. *Computer Methods in Applied Mechanics and Engineering*, vol. 32, pp. 199–259, 1982.
[2] T. J. Hughes, L. P. Franca, and M. Balestra. A new finite element formulation for computational fluid dynamics: V. circumventing the babuška-brezzi condition: a stable petrov-galerkin formulation of the stokes problem accommodating equal-order interpolations. *Computer Methods in Applied Mechanics and Engineering*, vol. 59, pp. 85–99, 1986.
[3] T. J. Hughes, L. Mazzei, and K. E. Jansen. Large eddy simulation and the variational multiscale method. *Computing and Visualization in Science*, vol. 3, pp. 47–59. usa espaço-tempo, 2000.
[4] T. J. Hughes, G. R. Feijóo, L. Mazzei, and J. B. Quincy. The variational multiscale method—a paradigm for computational mechanics. *Computer Methods in Applied Mechanics and Engineering*, vol. 166, pp. 3–24, 1998.
[5] T. J. Hughes. Multiscale phenomena: Green's functions, the dirichlet-to-neumann formulation, subgrid scale models, bubbles and the origins of stabilized methods. *Computer Methods in Applied Mechanics and Engineering*, vol. 127, pp. 387–401, 1995.
[6] O. Reynolds. Iv. on the dynamical theory of incompressible viscous fluids and the determination of the criterion. *Philosophical Transactions of the Royal Society of London. (A.)*, vol. 186, pp. 123–164, 1895.
[7] J. Smagorinsky. General circulation experiments with the primitive equations: I. the basic experiment. *Monthly weather review*, vol. 91, n. 3, pp. 99–164, 1963.
[8] C. S. Peskin. The immersed boundary method. *Acta Numerica*, vol. 11, pp. 479–517, 2002.
[9] T. E. Tezduyar, S. Sathe, J. Pausewang, M. Schwaab, J. Christopher, and J. Crabtree. Interface projection techniques for fluid–structure interaction modeling with moving-mesh methods. *Computational Mechanics*, vol. 43, pp. 39–49, 2008.
[10] J. Donea, S. Giuliani, and J. P. Halleux. An arbitrary lagrangian-eulerian finite element method for transient dynamic fluid-structure interactions. *Computer Methods in Applied Mechanics and Engineering*, vol. 33, pp. 689–723, 1982.
[11] J. W. D. Fernandes, H. B. Coda, and R. A. K. Sanches. Ale incompressible fluid–shell coupling based on a higher-order auxiliary mesh and positional shell finite element. *Computational Mechanics*, vol. 63, pp. 555–569, 2019.
[12] R. A. Sanches and H. B. Coda. Unconstrained vector nonlinear dynamic shell formulation applied to fluid structure interaction. *Computer Methods in Applied Mechanics and Engineering*, vol. 259, pp. 177–196, 2013.
[13] H. B. Coda and R. R. Paccola. An alternative positional fem formulation for geometrically non-linear analysis of shells: Curved triangular isoparametric elements. *Computational Mechanics*, vol. 40, pp. 185–200, 2007.
[14] T. E. Tezduyar, S. Mittal, S. E. Ray, and R. Shih. Incompressible flow computations with stabilized bilinear and linear equal-order-interpolation velocity-pressure elements. *Computer Methods in Applied Mechanics and Engineering*, vol. 95, pp. 221–242, 1992.
[15] Streamline upwind/petrov-galerkin formulations for convection dominated flows with particular emphasis on the incompressible navier-stokes equations. *Computer Methods in Applied Mechanics and Engineering*, vol. 32, pp. 199–259, 1982.
[16] T. E. Tezduyar. Computation of moving boundaries and interfaces and stabilization parameters. *International Journal for Numerical Methods in Fluids*, vol. 43, pp. 555–575, 2003.
[17] Y. Bazilevs, K. Takizawa, and T. E. Tezduyar. *Computational Fluid–Structure Interaction*. Wiley, 2013.
[18] K. E. Jansen, C. H. Whiting, and G. M. Hulbert. A generalized-α method for integrating the filtered navier–stokes equations with a stabilized finite element method. *Computer Methods in Applied Mechanics and Engineering*, vol. 190, pp. 305–319, 2000.
[19] T. Richter. *Fluid-structure Interactions*, volume 118. Springer International Publishing, 2017.
[20] A. Masud, M. Bhanabhagvanwala, and R. A. Khurram. An adaptive mesh rezoning scheme for moving boundary flows and fluid–structure interaction. *Computers & Fluids*, vol. 36, pp. 77–91, 2007.
[21] H. Kanchi and A. Masud. A 3d adaptive mesh moving scheme. *International Journal for Numerical Methods in Fluids*, vol. 54, pp. 923–944, 2007.
[22] W. A. Wall and E. Ramm. Fluid-structure interaction based upon a stabilized (ale) finite element method. In S. Idelsohn, E. Oñate, and E. Dvorkin, eds, *Computational Mechanics: New Trends and Applications*, pp. 1–20, Barcelona, Spain. CIMNE, 1998.